International Journal of Science and Research (IJSR)
ISSN (Online): 2319-7064
Index Copernicus Value (2015): 78.96 | Impact Factor (2015): 6.391

Intelligent Mechanical Sensorless MPPT Control for Wind Energy Systems

A. J. Gaikwad[1], P. C. Tapre[2]

[1]PG Student, Department of Electrical Engg. S.N.D.COERC, Nasik, Maharashtra, India

[2]Professor, H.O.D, Department of Electrical Engg. S.N.D.COERC, Nasik, Maharashtra, India

Abstract: ***Wind energy systems (WESs) are usually equipped with mechanical sensors to measure wind speed, rotor shaft speed, and generator rotor position/speed for system monitoring, control, and protection. The use of these sensors increases cost, size, weight, and hardware wiring complexity and reduces reliability of WESs. The problems incurred in using mechanical sensors can be solved through mechanical sensorless control. This paper presents the principles of mechanical sensorless maximum power point tracking (MPPT) control for WESs based on an overview of existing work on the subject. Several intelligent mechanical sensorless control algorithms for WESs are presented, including: 1) a hill-climb search (HCS)-based wind speed sensor-less MPPT control algorithm, 2) various artificial neural network (ANN)-based wind speed sensorless MPPT control algorithms, and 3) an ANN-sliding mode observer(SMO)-based wind speed, generator rotor position and shaft speed sensorless MPPT control algorithm. The effectiveness ofthese intelligent mechanical sensorless MPPT control algorithms are demonstrated by computer simulations as well as experiments on practical WESs.***

Keywords: Artificial neural network (ANN), intelligent control, maximum power point tracking (MPPT), sensorless control, wind energy system (WES).

1. Introduction

Traditionally, the oscillatory behavior of power systems has been dominated by the electromechanical interactions between the synchronous generators through the network. As the generation of power from wind energy conversion systems (WECS) using induction generators is increasing significantly, it is important to assess the impact of this type of asynchronous generation on the system stability and vice versa. The dynamic behavior of the doubly fed induction generator (DFIG) has been investigated by various authors. The majority of these studies are based on time-domain simulations to show the impact on power system dynamics the performance of decoupled control and maximum power tracking the response to grid disturbances the fault ride through behaviour the control methods to make the DFIG behave like a synchronous generator etc. Time-domain studies offer a direct appreciation of the dynamic behavior in terms of visual clarity. However, they are not able to identify and quantify the cause and nature of interactions and problems. This complementary information can be obtained with eigen value studies. Such studies have been carried out earlier for fixed-speed induction generators in WECS applications and variable speed induction machines in slip-energy recovery drive applications.In this paper, the grid-connected DFIG is studied. The single-machine infinite-bus (SMIB) approach is followed.

2. Traditional MPPT Control

A more detailed block diagram of proposed wind power generation system is shown in Fig.1. A PM motor is used as wind generator due to its advantages such as high efficiency and small size. The PM motor is droved by a three-phase inverter to generate 350V direct current power, and a Hitachi digital signal processor (DSP) controls the inverter to accomplish the maximum power point tracking. Because of the balance of the motor three-phase currents, only two of them are measured and they are controlled by DSP to generate power. Speed of generator is measured by using photo pulses encode and it is also controlled by DSP to get optimum rotating speed. The three-phase inverter is controlled by pulse width modulation (PWM). There is also an I/O interface to manipulate generation system such as Stop, run and reset etc.

3. HCS-Based Wind Speed Sensorless MPPT Control

Fig. 1 illustrates a WTG controlled by an HCS-based wind speed senseless MPPT algorithm. Based on the shaft speed (ωt) and output electrical power (Pe) of the WTG, the HSC algorithm generates the shaft speed command (ωt*), which is used by the feedback controller of the power electronic converter to regulate the shaft speed of the generator. The principle of the HCS algorithm is shown in Fig. 2. In this method, at a certain wind speed condition, the shaft speed command is continuously adjusted by a constant increment/ decrement of dωt in each search step. As a result, the output electrical power changes by dPe. If dPe/dωt > 0, ωt* keeps increasing; otherwise, if dPe/dωt < 0, ωt* keeps decreasing until the MPP is located. The corresponding shaft speed command is the optimal value t,opt ω∗ . If the wind speed vw varies slowly and the time interval of the search step is sufficiently small, the shaft speed will be always controlled around the optimal value.

4. PSF-Based Wind Speed Sensorless MPPT Control

Fig. 3 illustrates a WTG controlled by a PSF-based wind speed senseless MPPT algorithm, where the optimal shaft speed/power command corresponding to the MPP of the WTG is determined directly or indirectly from the output power and shaft speed of the WTG by utilizing the power-shaft speed wind speed wind speed characteristics of the WTG. The optimal shaft speed/power command is then used

by the feedback controller of the power electronic converter to control the shaft speed/power of the generator for MPPT.

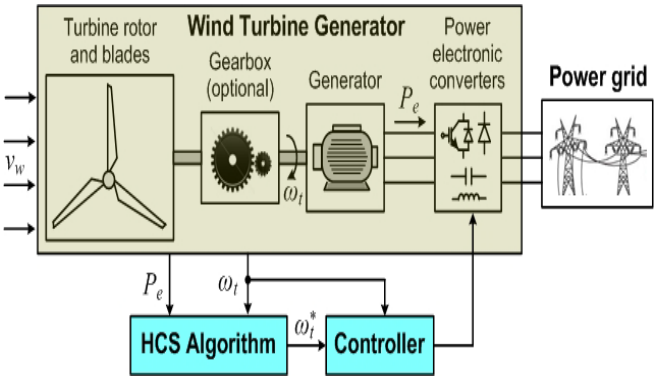

Figure 1: HCS-based wind speed sensorless MPPT control for a WTG.

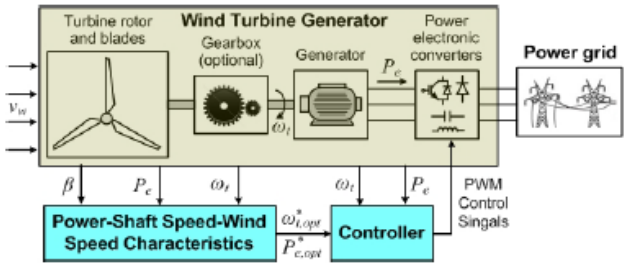

Figure 2: The principle of the HCS algorithm.

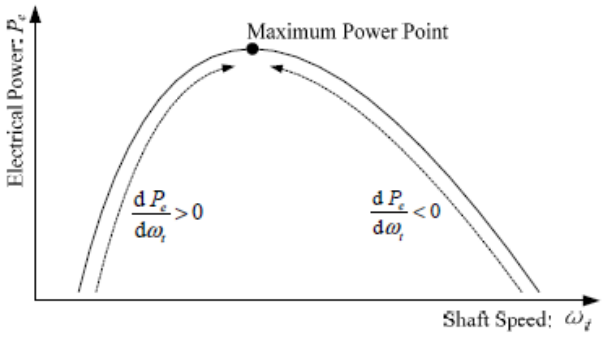

Figure 3: PSF-based wind speed sensorless MPPT control for a WTG

A. The Principle of PSF-Based MPPT

For a WTG system, the electrical power generation from wind energy can be described by the process in the flow chart in Fig. 4. The conversion of wind energy (Pw) to turbine mechanical power (Pm) is called wind turbine aerodynamics, where the turbine mechanical power Pm is represented as an on linear function of the wind speed vw, turbine shaft speed ωt, and blade pitch angle β. The mechanical power is transferred from the turbine to the generator (Pin) through the shaft system dynamics. The generator converts mechanical power into electrical power (Pe). The losses (Ploss) of the whole process are referred to the generator side. The output electrical power Pe of the generator is measured. Therefore, if developing an inverse model from Pe to vw by using the information of ωt, and β, then the wind speed can be estimated from the measured output electrical power. Once the estimated wind speed ˆw v is obtained, the optimal shaft speed command t, opt ω, which corresponds to the MPP, can be determined, where λopt and R are the optimal tip speed ratio (a constant at a fixed blade pitch angle) and wind turbine rotor radius, respectively. Since the wind speed may vary fast and

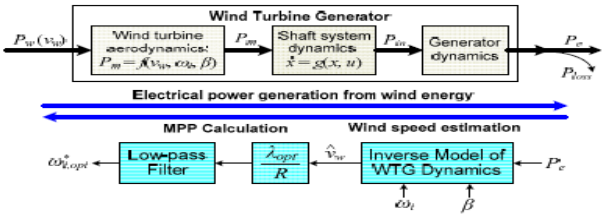

Figure 4: The principle of PSF-based MPPT

The inverse model used to estimate wind speed from (Pe,ωt, β) can be implemented by using a look-up table, polynomial-based curve fitting, or ANN-based nonlinear approximation. The first two methods are only able to provide a static mapping between (Pe, ωt, β) and windspeed while neglecting the dynamics of the WTG system shown in Fig. 4.On the contrary, the ANN-based models can estimate wind speed from (Pe, ωt, β) while taking into account the dynamics of the WTG system. Therefore, several ANN-based models are designed in the following section for wind speed estimation. Moreover, instead of determining the optimal shaft speed command indirectly using the estimated wind speed, an ANN-based model can be designed to obtain the optimal shaft speed command directly from (Pe, ωt, β) without the need of wind speed estimation.

B. PSF-Based MPPT via Wind Speed Estimation

Two ANN-based models are designed to estimate the wind speed from (Pe, ωt, β). One uses a three-layer Gaussian radial basis function network (GRBFN). while the other uses an echo state network (ESN). GRBFN-Based Wind Speed Estimation: A GRBFN is designed to perform a nonlinear inverse modeling of the WTG dynamics to estimate the wind speed, as shown in Fig. 5. The overall input-output mapping for the GRBFN is given by:

$$\hat{v}_w = b + \sum_{j=1}^{h} v_j \exp\left(-\frac{\|x - C_j\|^2}{\sigma_j^2}\right) \quad \text{.....(1)}$$

where x = [Pe, ωt, β] is the input vector; Cj∈ R^n and σj∈ R are the center and width of the j^{th} RBF unit in the hidden layer, respectively; h is the number of RBF units; b and v_j are the bias term and the weight between hidden and output layers, respectively; and vˆw is the output of the GRBFN that represents the estimated wind speed. The parameters of the GRBFN, including the number of RBF units, the RBF centers and width, and the output weights and bias term, are determined by an offline training and optimization using a training data set generated from the WTG dynamic characteristics, which can be obtained from simulation and/or experiment. This data set covers the entire operating range of the WTG. Once trained, the parameters of the GRBFN are then fixed for real-time wind speed estimation. ESN-Based Wind Speed Estimation: An ESN is also designed to provide an inverse model of WTG dynamics to estimate wind speed in real time from (Pe, ωt, β), as shown in Fig. 6. The ESN is a novel approach for designing and supervised training of recurrent neural networks (RNNs). An ESN consists of a large, fixed RNN called dynamical reservoir (DR), which can be excited by suitably presented

input and/or fed-back output. The desired output dynamics are then obtained by training the connection weights from the DR to the output only; while all other connection weights are fixed during the training. In this application, the input and output activations of the ESN at the time step k are u(k) = [Pe(k),ωt(k), β(k)] and y(k) = vˆw (k) , respectively. The activation functions of the internal and output units are both sigmoid functions described by .

$$f(z) = \frac{1}{1+e^{-z}} \quad \text{.....(2)}$$

5. Rotor Position/Speed Sensorless Control For Direct-Drive PMSG Wind Turbines

In a direct-drive PMSG wind turbine, the information of the PMSG rotor position angle θr and shaft speed ωt is needed for MPPT control. In this section, a sliding-mode observer (SMO) is designed to estimate the PMSG rotor position [6], which is then used to calculate the turbine shaft speed.A. SMO-Based Rotor Position Estimation The dynamic equations of a nonsalient-pole PMSG in the

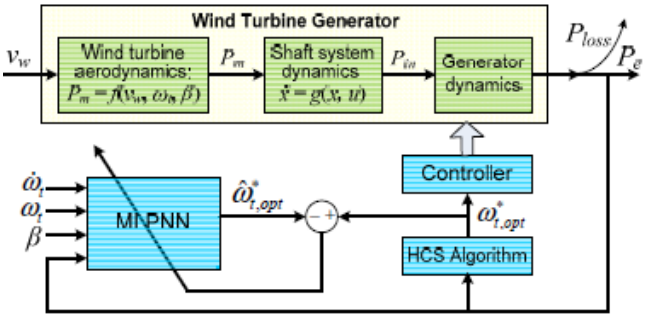

Figure 7: MLPNN-based MPPT.

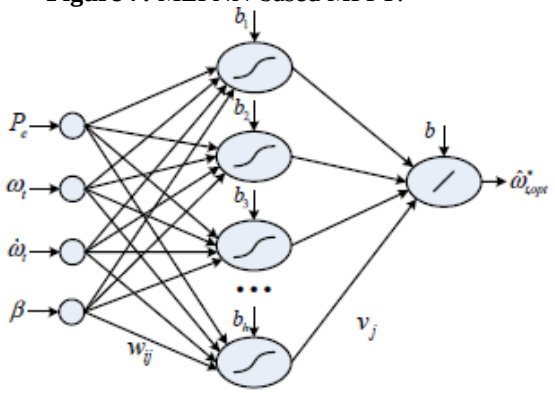

Figure 8: MLPNN-based optimal shaft speed command Determination

$$\dot{i}_{\alpha\beta} = A \cdot i_{\alpha\beta} + B \cdot (v_{\alpha\beta} - e_{\alpha\beta}) \quad \text{.....(3)}$$

where vαβ, iαβ, and eαβ are the stator voltages and currents andback EMF in the stationary referenceframe, respectively; and

$$A = \begin{bmatrix} \frac{-R_s}{L_s} & 0 \\ 0 & \frac{-R_s}{L_s} \end{bmatrix}, \quad B = \begin{bmatrix} \frac{1}{L_s} & 0 \\ 0 & \frac{1}{L_s} \end{bmatrix}, \quad i_{\alpha\beta} = \begin{bmatrix} i_\alpha \\ i_\beta \end{bmatrix}, \quad v_{\alpha\beta} = \begin{bmatrix} v_\alpha \\ v_\beta \end{bmatrix},$$

$$e_{\alpha\beta} = \begin{bmatrix} e_\alpha \\ e_\beta \end{bmatrix} = K_e \cdot \omega_t \cdot \begin{bmatrix} -\sin(\theta_r) \\ \cos(\theta_r) \end{bmatrix} \quad \text{..(4)}$$

where Rs and Ls are the resistance and inductance of the stator windings, respectively; and Ke is a back EMF constant. Then an SMO can be designed as follows to estimate iαβ.

$$\hat{i}_{\alpha\beta} = A \cdot \hat{i}_{\alpha\beta} + B \cdot v_{\alpha\beta} + k\,\mathrm{sgn}(\hat{i}_{\alpha\beta} - i_{\alpha\beta})$$

$$Z_{\alpha\beta} = k\,\mathrm{sgn}(\varepsilon_{is}) = k\,\mathrm{sgn}(\hat{i}_{\alpha\beta} - i_{\alpha\beta}) \quad \text{.....(5)}$$

where iαβ $ is the estimated value of iαβ; Zαβ is the switching signal; sgn(·) is the sign function; k is the switching gain of the SMO. Fig. 9 shows the schematic of the SMO-based rotor position estimation algorithm, where êαβ is the estimated back EMF, which is obtained by a low-pass filter from the switching signal Zαβ; and ˆ r θ is the estimated rotor position angle.

The rotor position is then obtained as:

$$\hat{\theta}_r = -\tan^{-1}\left(\frac{\hat{e}_\alpha}{\hat{e}_\beta}\right) \quad \text{.....(6)}$$

6. Conclusion

This paper has provided an overview of existing work on mechanical sensorless MPPT control for variable-speed WESs. Several intelligent algorithms have been presented for mechanical sensorless MPPT control of WESs. These include a HCS-based wind speed sensor-less MPPT control algorithm, several ANN-based wind speed sensorless MPPT control algorithms, and an ANN-SMO-based wind speed and rotor position/speed sensorless MPPT control algorithm for PMSG wind turbines.

References

[1] "20% wind energy by 2030: Increasing wind energy's contribution to U.S. electricity supply," U.S. Department of Energy, July 2008.
[2] "Focus on 2030: EWEA aims for 22% of Europe's electricity by 2030," Wind Directions, pp. 25-34, Nov./Dec. 2006.
[3] J. Ribrant and L. M. Bertling, "Survey of failures in wind power systems with focus on Swedish wind power plants during 1997-2005," IEEE Trans. Energy Conversion, vol. 22, no. 1, pp. 167-173, Mar. 2007.
[4] W. Qiao, W. Zhou, J. M. Aller, and R. G. Harley, "Wind speed estimation based sensorless output maximization control for a wind turbine driving a DFIG," IEEE Trans. Power Electronics, vol. 23, no. 3, pp. 1156-1169, May 2008.
[5] W. Qiao, X. Yang, and X. Gong, "Wind speed and rotor position sensorless control for direct-drive PMG wind turbines," IEEE Trans. Industry Applications, vol. 48, no. 1, Jan/Feb 2012, in press.
[6] W. Qiao, X. Gong, and L. Qu, "Output maximization control for DFIG wind turbines without using wind and shaft speed measurements," in Proc. IEEE ECCE 2009, San Jose, CA, Sept. 20-24, 2009, pp. 404-410.
[7] X. Yang, X. Gong, and W. Qiao, "Mechanical sensorless maximum power tracking control for direct-

drive PMSG wind turbines," in Proc.IEEE ECCE 2010, Atlanta, GA, Sept. 12-16, 2010, pp. 4091-4098.

[8] H. Li, K. L. Shi, and P. G. McLaren, "Neural-network-based sensorless maximum wind energy capture with compensated power coefficient,"IEEE Tran. Industry Applications, vol. 41, no. 6, pp. 1548-1556, Nov./Dec. 2005.

[9] B. Boukhezzar and H. Siguerdidjane, "Nonlinear control of variable speed wind turbines without wind speed measurement," in Proc. 44th IEEE Conference on Decision and Control, Seville, Spain, Dec. 12-15,2005, pp. 3456-3461.

[10] H. Jaeger, "The 'echo state' approach to analysing and training recurrent neural networks," GMD Report 148, German National Research Center for Information Technology, 2001.

[11] K. Tan and S. Islam, "Optimal control strategies in energy conversion of PMSG wind turbine system without mechanical sensors," IEEE Trans. Energy Conversion, vol. 19, no. 2, pp. 392-399, Jun. 2004.